Lowering barriers in surface reactions through concerted reaction mechanisms

Sung Sakong,[1] Christian Mosch,[2] Ariel Lozano,[3] H. Fabio Busnengo,[3] and Axel Groß[2,*]

[1]*Fakultät für Physik and Center for Nanointegration (CeNIDE), Universität Duisburg-Essen, D-47048 Duisburg/Germany*

[2]*Institut für Theoretische Chemie, Universität Ulm, D-89069 Ulm/Germany*

[3]*Instituto de Física de Rosario, Consejo Nacional de Investigaciones Científicas y Técnicas (CONICET) and Universidad Nacional de Rosario, Rosario, Argentina*

Any technologically important chemical reaction typically involves a number of different elementary reaction steps consisting of bond-breaking and bond-making processes. Usually one assumes that such complex chemical reactions involving several bond-breaking and bond-making steps occur in a step-wise fashion where one single bond is made or broken at a time. Here we show, using first-principles calculations based on density functional theory, that the barriers of rate-limiting steps for technologically relevant surface reactions can be significantly reduced if concerted reaction mechanisms are taken into account.

Keywords: Surface chemistry, reaction mechanisms, density functional calculations, methanol, hydrogen

I. INTRODUCTION

Chemical reactions at surfaces are of outstanding technological importance since they correspond to the basic processes occuring in heterogeneous catalysis, corrosion, sensing, etc. They also play a crucial role in the energy storage and conversion in renewable energy systems [1]. Hence an understanding of the basic mechanisms occuring in surface reactions is not only interesting from a fundamental point of view, it is also very beneficial from a technological point of view. In the modeling of such surface reactions it is usually assumed that the bond-breaking and bond-making processes involving the reactants occur in a consecutive fashion (see, e.g., [2]).

Still, it is well-known that chemical reactions can also proceed in a concerted fashion which means that bond breaking and bond making occurs simultaneously, for example in the so-called S_N2 reactions [3]. Yet, there are usually severe symmetry constraints involved in concerted reaction mechanisms, as for example expressed in the Woodward-Hoffman rules [4] which state that the symmetry of the wave function shall remain unchanged upon this reaction.

However, in surface reactions the configurations often exhibit little symmetry which is also true for the involved electronic states. Here we show, using first-principles calculations based on density functional theory (DFT), that the barriers of rate-limiting steps for technologically relevant surface reactions can be significantly reduced if concerted reaction mechanisms are taken into account. We will illustrate this using the reaction paths of two technologically relevant reactions as examples, namely the methanol synthesis on copper and the subsurface penetration of hydrogen on palladium, which are in fact both of high relevance for our understanding of elementary processes in chemical energy storage and conversion. All total energy calculations presented in this paper are based on periodic DFT calculations as implemented in the VASP code [5]. For further computational details, we refer to the supporting information.

II. COMPUTATIONAL METHODS

Density functional theory (DFT) calculations have been performed using the Vienna *ab initio* simulation package (VASP) [5]. The exchange-correlation effects are described within the framework of generalized gradient approximation (GGA) using Perdew-Berke-Ernzelhoff (PBE) functional [6]. The ionic cores were represented by projector augmented wave (PAW) potentials [7] as constructed by Kresse and Joubert [8]. The metal substrates were represented by four- and five-layer slabs. The integration over the first Brillouin zone in reciprocal space was replaced by a sum over a sufficiently large set of k-points.

The reaction barriers are evaluated by using reversible work transition state theory (rwTST) which is implemented into VASP by Jónsson et al. [9]. In practice, we have used the nudged elastic band (NEB) method [10] to find the minimum energy paths and the activation barrier.

III. METHANOL SYNTHESIS

Methanol synthesis is of significant importance because it is the basis for many chemicals. Furthermore, methanol is considered as a potential fuel in the hydrogen technology. Industrially, methanol is produced by the hydrogenation of carbon dioxide and together with the water gas shift reaction from natural gas on oxide supported Cu/ZnO catalysts [11–13]. Interestingly enough, the exact reaction mechanism leading to methanol formation is still debated in spite of the importance of this

*Supporting information for this article is available on the WWW under http://dx.doi.org/10.1002/cphc.2009xxxxx.

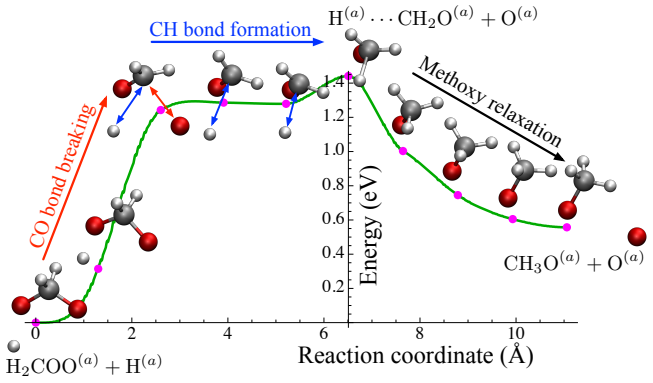

FIG. 1: Reaction path for the conversion of $H_2COO^{(a)} + H^{(a)}$ into $CH_3O^{(a)} + O^{(a)}$ on a hydrogen-covered Cu(110) surface.

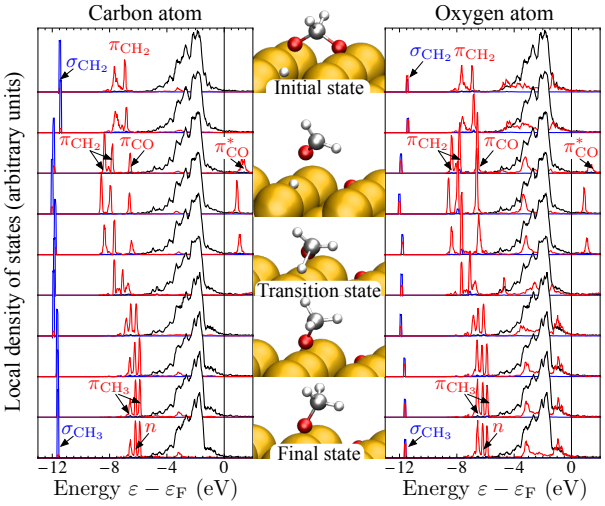

FIG. 2: Local density of states at the carbon and the oxygen atom of the resulting methoxy atom along the reaction path shown in Fig. 1. In addition, in both panels the averaged local density of states of the first layer copper atoms is plotted in black.

reaction. Since it is assumed that metallic Cu particles rather than ZnO are the active material in methanol synthesis [14–16], several surface science studies have been performed on Cu single crystal surfaces in order to elucidate the reaction mechanism in methanol synthesis [17] and in the reverse process, the methanol oxidation [18]. Here we concentrate on the Cu(110) surface which represents a model system for the interaction of methanol with Cu [18].

Experiments indicate that CO_2 is the primary source in the methanol production [16]. Therefore we have focused in our computational study on the reaction path starting with the interaction of CO_2 with hydrogen dissociatively adsorbed on Cu(110). Note that mechanistic details of the water gas shift reaction $CO + H_2O \rightarrow CO_2 + H_2$ have been adressed previously in theoretical studies [19, 20]. According to our analysis, the initial reaction steps lead to the formation of adsorbed dioxymethylene ($H_2COO^{(a)}$) on Cu(110) (see Figs.1 and 2 for an illustration), where the superscript (a) indicates that the molecule is adsorbed on the surface. In a previous DFT study [20], on Cu(1111) much lower barriers were found for formic acid (HCOOH) formation from formate ($E_a = 0.91\,\mathrm{eV}$) than for desoxymethylene formation ($E_a = 1.59\,\mathrm{eV}$). However, on Cu(110) the barrier for desoxymethylene formation is much lower ($E_a = 0.95\,\mathrm{eV}$). Furthermore, we note that isotopic labeling studies showed that methanol could not be synthesized by HCOOH hydrogenation [21]. Hence we focus in our study on the reaction pathway involving desoxymethylene as a reaction intermediate.

As for the further reaction mechanism, assuming a stepwise mechanism first involving a CO bond breaking and then a hydrogenation step would lead to the following reaction scenario:

$$H_2COO^{(a)} + H^{(a)} \longrightarrow CH_2O^{(a)} + OH^{(a)}, \quad (1)$$

$$CH_2O^{(a)} + H^{(a)} \longrightarrow CH_3O^{(a)} \quad (2)$$

However, the first reaction step (1) is hindered by a significant barrier of 1.8 eV on Cu(110) according to our calculations. Now quite some time ago it was proposed [17] that the methanol synthesis on Cu might involve a reaction step

$$H_2COO^{(a)} + H^{(a)} \longrightarrow CH_3O^{(a)} + O^{(a)}. \quad (3)$$

which corresponds to a combination of C-O bond scission and a hydrogenation step. This reaction step was proposed purely because of kinetic reasons in order to reproduce the experimentally observed reaction order, but no mechanistic model in terms of the microscopic reaction mechanism was given. In a recent DFT study of the methanol synthesis on Cu(111), however, such a concerted mechanism could not be identified [20]. Yet, based on a comparison of the DFT results with binding energies derived from microkinetic modeling the authors concluded that Cu(111) might not provide a suitable representation of the active site for methanol synthesis. It might also well be that the proper initial configuration of the co-adsorbates on the surface has been missed, as we will argue below.

Using an unbiased automatic transition state search routine, the nudged elastic band method (NEB) [10], we have looked for the most favorable reaction path connecting the initial state of dioxymethylene in the presence of adsorbed hydrogen atoms (see Fig. 1). As the first step, we carefully determined the energetically most favorable configuration of the hydrogen atoms in the vicinity of the adsorbed dioxymethylene molecule. Along the reaction path, first the dioxymethylene molecule is reoriented and one oxygen atom of the molecule moves from a two-fold bridge-like site towards a quasi-threefold hollow site at the trough of the (110) surface. The corresponding distortion of the molecule is associated with a large energy cost of more than 1 eV. Before the tran-

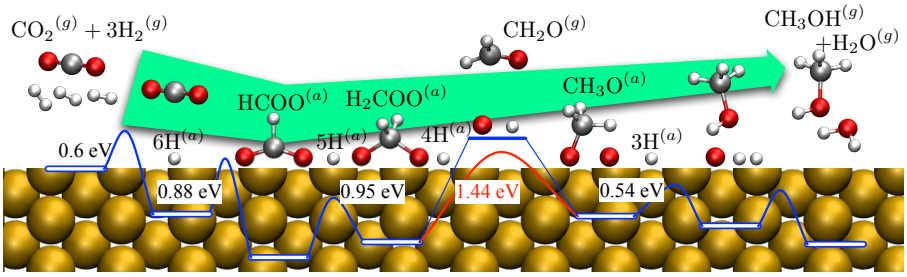

FIG. 3: Reaction scheme for the methanol synthesis on hydrogen-covered Cu(110).

sition state, there is a plateau in the potential energy which, however, does not correspond to an intermediate state. At the transition state, one C-O bond is already significantly elongated and the CH_2 group starts to turn. While the one C-O bond is further elongated, a hydrogen atom from the Cu surface is forming a C-H bond, thus turning the evolving formaldehyde (CH_2O) into the methoxy radical (CH_3O). The energy of the transition state is about 1.4 eV, i.e., 0.4 eV lower than the barrier for mechanism involving two consecutive reaction steps. Note that such a reduction in the barrier height leads to an increase in the rate constant of the reaction of 2–3 orders of magnitude at 600-900 K, the temperature range in which methanol is typically synthesized [22].

In order to determine the electronic factors underlying this reduction in the barrier height, we have analyzed the local density of states (LDOS) of the reacting complex along the reaction path for the concerted reaction (3) (see Fig. 2). At the transition state where the C-O bond is already significantly extended, there is a strong rearrangement of the electronic states with an anti-bonding CO π^* appearing just above the Fermi energy whereas the electronic distribution just before and after the transition state look rather alike. In the framework of the frontier orbital concept of Fukui [23], the lowest unoccupied molecular orbital (LUMO) close to the Fermi energy at the transition state leads to a rather reactive complex. One can also put it differently: Directly after the C-O bond breaking the missing bonding partner O is replaced by the nearest hydrogen atom resulting in an equivalent coordination of the carbon atom.

It is important to note that another consequence of this concerted reaction mechanism is that the formation of formaldehyde (CH_2O) is avoided which is only weakly bound to Cu at the temperature methanol synthesized [24, 25]. It corresponds to a volatile product which under reaction conditions would immediately desorb. This also means that the methanol synthesis would remain incomplete if formaldehyde was formed. Furthermore, this also rationalizes why formaldehyde can not be produced industrially through the oxidation of CO or CO_2 [17], rather, it is formed through the partial oxidation of methanol [18].

The final step after the methoxy formation, the recombinative desorption of methanol and water, is hindered by a relatively small barrier of 0.5 eV. The calculated overall reaction for the methanol synthesis on H-covered Cu(110) is summarized in Fig. 3. It becomes apparent that the conversion of adsorbed dioxymethylene has the highest barrier of all involved reaction steps. This means that it corresponds to the rate-limiting step which is significantly lowered by taking into account the concerted reaction mechanism.

Interestingly enough, methanol has not been observed as a reaction product of the electrochemical reduction of CO_2 at Cu electrodes, but rather methane [26]. It has recently be suggested that this might be due to the fact that in heterogeneous catalysis the hydrogen addition comes from coadsorbed hydrogen atoms whereas in electrocatalysis the protons come from solution [27]. Therefore an entirely different reaction mechanism is operative.

IV. HYDROGEN SUBSURFACE PENETRATION

As a second example, we consider the subsurface penetration of hydrogen on Pd(100). Currently, there has been a renewed interest in the hydrogen absorption in metals [28–30] in the context of the hydrogen technology. Due to its high specific mass, Pd is no longer considered as a candidate material for hydrogen storage. Still, it is considered to be *the* model system for the study of hydrogen absorption. Furthermore, thin capping palladium films are typically used as hydrogen-insertion promoters for complex hydrides formed by light elements [31]. In addition, subsurface penetration of hydrogen in Pd nanoparticles might be the crucial promoter for the olefin hydrogenation [32].

According to experiments, hydrogen first adsorbs *on* the Pd surface before bulk absorption starts [33]. Only after the surface is covered by hydrogen, subsurface penetration occurs, but then rather easily. This is at variance with the accepted notion that the hydrogen penetration into the Pd bulk is hindered by barriers of considerable height [28]. Therefore, it is of interest whether the high barrier for H subsurface penetration is influenced by the presence of hydrogen adsorbates through, e.g., a defect-mediated [34] or a concerted reaction mechanism.

Static DFT calculations have confirmed the prefer-

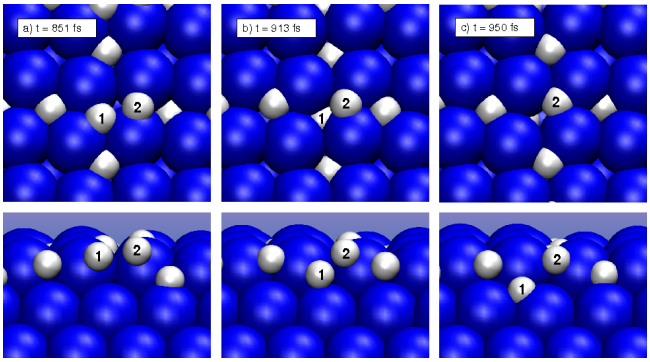

FIG. 4: Top and side view of snapshots of the subsurface penetration of hydrogen on Pd(100) taken from an ab initio molecular dynamics simulation at $t = 851\,\mathrm{fs}$ (a), $t = 913\,\mathrm{fs}$ (a) and $t = 950\,\mathrm{fs}$ (a). The H_2 molecule was impinging on hydrogen-covered Pd(100) surface with a coverage of $\Theta_H = 0.5$ within a (3×2) symmetry. The two hydrogen atoms participating in the subsurface penetration have been labeled by numbers.

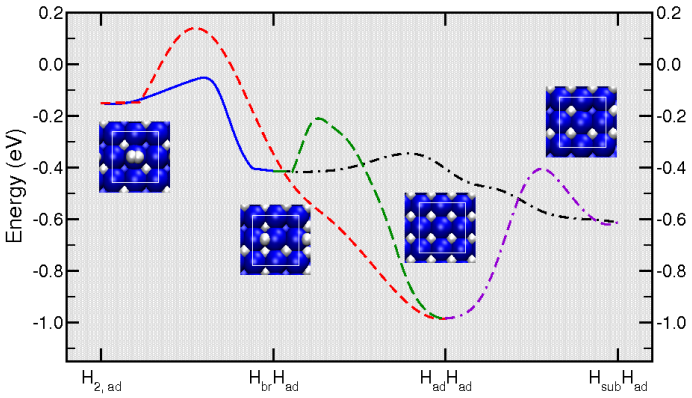

FIG. 5: Reaction scheme for the hydrogen subsurface penetration upon H_2 adsorption at $c(2 \times 2)$H/Pd(100). The configuration $H_{2,ad}$ corresponds to a molecular precursor at the top site within the (2×2) surface unit cell which is indicated by the white boxes. In $H_{br}H_{ad}$ one of the two hydrogen atoms is at the hollow adsorption site, the other one at the bridge site, in $H_{ad}H_{ad}$ all hydrogen atoms are at their hollow adsorption site, and in $H_{ad}H_{ad}$ one of the hydrogen atoms is in the subsurface site.

ential occupation of adsorption sites on the surface by demonstrating that hydrogen subsurface absorption is energetically less favorable than adsorption on the surface [35]. Since possible concerted reaction mechanisms are sensitive to the initial configuration, *ab initio* molecular dynamics (AIMD) simulations of the H_2 dissociative adsorption on hydrogen-precovered Pd(100) have been employed [36–38] for an unbiased search of concerted reactions for varying hydrogen coverages.

Besides of hydrogen adsorption and diffusion on the surface, frequently another event was observed in the AIMD simulations, namely a subsurface penetration of a hydrogen atom involving another hydrogen atom at an adjacent bridge-site in a concerted fashion. Snapshots of this process on a hydrogen-covered Pd(100) surface with an initial coverage of $\Theta_H = 0.5$ monolayer within a (3×2) unit cell are shown in Fig. 4 in a top and in a side view, an animation of this process is provided in the Supporting Information as Supplementary Movie S1. Note that the coverage is defined with respect to the number of Pd atoms in the surface.

In addition to adsorbed hydrogen atoms at four-fold hollow sites, there is another hydrogen atom adsorbed at a bridge site (labeled number 2 in Fig. 4) surrounded by filled four-fold hollow sites (Fig. 4a). Then the central H atom at the four-fold hollow site (labeled number 1) starts to propagate towards a subsurface site. At the same time, hydrogen atom 2 from the adjacent bridge site moves towards the four-fold hollow site that is about to be emptied (Fig. 4b). Thus, in a combined bond-making/bond breaking process, the one hydrogen atom enters the subsurface site while the four-fold hollow site is immediately filled by the hydrogen atom from the bridge site (Fig. 4c).

In order to analyze these observations, reaction paths for the hydrogen subsurface penetration, again using the NEB method [10], were determined. The results are summarized in Fig. 5. As an initial configuration, we started with a $c(2 \times 2)$H/Pd(100) surface, i.e. with a surface with an hydrogen coverage of $\Theta_H = 0.5$ but with no adjacent hydrogen vacancies, so that H_2 cannot dissociate directly [37]. On such a surface, above the Pd ontop site there is a molecular adsorption state, denoted by $H_{2,ad}$ in Fig. 5, which is stabilized by a rearrangement of the adjacent substrate atoms. The dissociation of H_2 into two next-nearest neighbor sites from this state is hindered by a barrier of about 0.3 eV (dashed red line in Fig. 5). At the fully hydrogen-covered Pd(100) surface, the subsurface penetration of a single hydrogen atom is hindered by a barrier of about 0.6 eV. This high barrier is due to the fact that the hydrogen atom has to propagate through a low-coordinated transition state also involving strain effects. Note also that the situation with all hydrogen atoms adsorbed *on* the surface is by 0.4 eV more stable compared to the situation with one hydrogen atom per (2×2) surface unit cell in the subsurface position.

However, from the molecular precursor state one of the two hydrogen atoms can adsorb in the four-fold hollow site (H_{ad}) whereas the other H atom can stay at the bridge site (H_{br}). This process is hindered by a barrier of only 0.1 eV (full blue line in Fig. 5). Even more importantly, the concerted subsurface penetration from this $H_{br}H_{ad}$ state with the H_{ad} atom entering the subsurface site and the H_{br} atom directly refilling the four-fold hollow site requires a barrier of only about 60 meV. In contrast, the propagation of the H_{br} atom into the empty four-fold hollow adsorption site is much less probable since it is hindered by a barrier of more than 0.2 eV.

In the concerted motion, the energy cost of the H atom going through the low-coordinated transition state to-

wards the subsurface site is compensated to a large extent by the energy gain when the bridge-site hydrogen atom enters the four-fold hollow site that is about to be emptied. The combined effect results in a concerted process that is hindered by a barrier of less than 0.1 eV. Rather similar results have also been found for an initial hydrogen coverage of $\Theta_H = 0.75$ (see Supplementary Fig. S2 and Movie S2). Such a concerted motion provides an explanation for the facile hydrogen subsurface penetration once the surface is almost covered by hydrogen [33]. This also indicates that there is no need to invoke any defect-mediated mechanism in order to explain the facile subsurface penetration [34].

V. CONCLUSIONS

In conclusion, we have demonstrated, based on periodic DFT calculations, that concerted reaction mechanisms can be a crucial part of technologically relevant reactions on surfaces. The driving force for these concerted reaction mechanisms is given by the fact that it is energetically favorable to create a new bond before the preceding bond-breaking process is fully completed which at surfaces is not hindered by symmetry selection rules. It is true that concerted reaction mechanisms in surface reactions have been identified before, for example in the methanol oxidation [39, 40]. On the other hand, sometimes concerted mechanisms could not be found in spite of significant efforts in exploring the relevant potential energy landscape [20]. However, it is important to note that a prerequisite for the occurrence of a concerted reaction mechanism is the availability of the second reaction partner. Hence, either a careful search for appropriate initial configuration is required, or an unbiased search using, e.g., AIMD simulations [36, 41] has to be performed. Without the proper initial configuration, there is no chance to identify concerted reaction mechanism which could lower a reaction barrier. It might well be that often the most favorable reaction mechanism has been missed in computational studies. This is also the reason why we believe that concerted reaction mechanisms are much more common than previously assumed.

This work has been supported by the German Science Foundation within the priority programme SPP 1091 (DFG contract GR 1503/12-2) and the research unit FOR 1376 (DFG contract GR 1503/21-1). Some of the calculations presented here were made possible through a grant of computer time at the John von Neumann Institute for Computing in Jülich. Additional computational resources have been provided by the bwGRiD project of the Federal State of Baden-Württemberg/Germany.

[1] Schlögl, R. *ChemSusChem* **2010**, *3*, 209–222.
[2] Mhadeshwar, A. B.; Vlachos, D. G. *J. Phys. Chem. B* **2005**, *109*, 16819–16835.
[3] Gronert, S. *Acc. Chem. Res.* **2003**, *36*, 848–857.
[4] Woodward, R. B.; Hoffmann, R. *J. Am. Chem. Soc.* **1965**, *87*, 395–397.
[5] Kresse, G.; Furthmüller, J. *Phys. Rev. B* **1996**, *54*, 11169.
[6] Perdew, J. P.; Burke, K.; Ernzerhof, M. *Phys. Rev. Lett.* **1996**, *77*, 3865.
[7] Blöchl, P. E. *Phys. Rev. B* **1994**, *50*, 17953.
[8] Kresse, G.; Joubert, D. *Phys. Rev. B* **1999**, *59*, 1758.
[9] Mills, G.; Jónsson, H.; Schenter, G. K. *Surf. Sci.* **1995**, *324*, 305.
[10] Henkelman, G.; Jónsson, H. *J. Chem. Phys.* **2000**, *113*, 9978.
[11] Chinchen, G. C.; Spencer, M. S.; Waugh, K. C.; Whan, D. A. *J. Chem. Soc. Faraday Trans. 1* **1987**, *83*, 2193 – 2212.
[12] Peppley, B.; Amphlett, J.; Kearns, L.; Mann, R. *Appl. Catal. A* **1999**, *179*, 31.
[13] Waugh, K. C. *Catal. Today* **1992**, *15*, 51.
[14] Chinchen, G. C.; Waugh, K. C.; Whan, D. A. *Appl. Catal.* **1986**, *25*, 101.
[15] Günter, M. M.; Ressler, T.; Bems, B.; Büscher, C.; Genger, T.; Hinrichsen, O.; Muhler, M.; Schlögl, R. *Catal. Lett.* **2001**, *71*, 37.
[16] Yoshihara, J.; Campbell, C. T. *J. Catal.* **1996**, *161*, 776.
[17] Rasmussen, P. B.; Holmblad, P. M.; Askgaard, T.; Ovesen, C. V.; Stoltze, P.; Nørskov, J. K.; Chorkendorff, I. *Catal. Lett.* **1994**, *26*, 373.
[18] Wachs, I. E.; Madix, R. J. *J. Catal.* **1978**, *53*, 208.
[19] Gokhale, A. A.; Dumesic, J. A.; Mavrikakis, M. *J. Am. Chem. Soc.* **2008**, *130*, 1402–1414.
[20] Grabow, L. C.; Mavrikakis, M. *ACS Catalysis* **2011**, *1*, 365.
[21] Ortelli, E.; Weigel, J.; Wokaun, A. *Catal. Lett.* **1998**, *54*, 41–48.
[22] Klier, K. *Adv. Catal.* **1982**, *31*, 243.
[23] Fukui, K. *Science* **1982**, *218*, 747.
[24] Sakong, S.; Groß, A. *J. Catal.* **2005**, *231*, 420.
[25] Sakong, S.; Groß, A. *J. Phys. Chem. A* **2007**, *111*, 8814.
[26] Hori, Y.; Murata, A.; Takahashi, R. *J. Chem. Soc., Faraday Trans. 1* **1989**, *85*, 2309–2326.
[27] Peterson, A. A.; Abild-Pedersen, F.; Studt, F.; Rossmeisl, J.; Nørskov, J. K. *Energy Environ. Sci.* **2010**, *3*, 1311–1315.
[28] Pundt, A.; Kirchheim, R. *Annu. Rev. Mater. Res.* **2006**, *36*, 555–608.
[29] Groß, A. *Surf. Sci.* **2012**, *606*, 690 – 691.
[30] Ferrin, P.; Kandoi, S.; Nilekar, A. U.; Mavrikakis, M. *Surf. Sci.* **2012**, *606*, 679 – 689.
[31] Isidorsson, J.; Giebels, I. A. M. E.; Arwin, H.; Griessen, R. *Phys. Rev. B* **2003**, *68*, 115112.
[32] Wilde, M.; Fukutani, K.; Ludwig, Wiebke Brandt, B.; Fischer, J.-H.; Schauermann, S.; Freund, H.-J. *Angew. Chem. Int. Ed.* **2008**, *47*, 9289.
[33] Muschiol, U.; Schmidt, P. K.; Christmann, K. *Surf. Sci.* **1998**, *395*, 182.
[34] Okuyama, H.; Siga, W.; Takagi, N.; Nishijima, M.; Aruga, T. *Surf. Sci.* **1998**, *401*, 344 – 354.
[35] Lischka, M.; Groß, A. *Phys. Rev. B* **2002**, *65*, 075420.

[36] Groß, A.; Dianat, A. *Phys. Rev. Lett.* **2007**, *98*, 206107.
[37] Lozano, A.; Groß, A.; Busnengo, H. F. *Phys. Rev. B* **2010**, *81*, 121402(R).
[38] Groß, A. *J. Chem. Phys.* **2011**, *135*, 174707.
[39] Greeley, J.; Mavrikakis, M. *J. Am. Chem. Soc.* **2004**, *126*, 3910–3919.
[40] Hartnig, C.; Spohr, E. *Chem. Phys.* **2005**, *319*, 185.
[41] Berkelbach, T. C.; Lee, H.-S.; Tuckerman, M. E. *Phys. Rev. Lett.* **2009**, *103*, 238302.

Supporting Information for

Lowering reaction barries is surface reactions through concerted reaction mechanisms

Sung Sakong,[1] Christian Mosch,[2] Ariel Lozano,[3] H. Fabio Busnengo,[3] and Axel Groß[2]

[1]*Fachbereich Physik, Universität Duisburg-Essen, D47048 Duisburg/Germany*
[2]*Institut für Theoretische Chemie, Universität Ulm, D-89069 Ulm/Germany*
[3]*Instituto de Física de Rosario, Consejo Nacional de Investigaciones Científicas y Técnicas (CONICET) and Universidad Nacional de Rosario, Rosario, Argentina*

(Dated: June 28, 2012)

This PDF includes

Supporting online material:
Hydrogen subsurface penetration on Pd(100) with $\Theta_H = 0.5$ coverage
Hydrogen subsurface penetration on Pd(100) with $\Theta_H = 0.75$ coverage

Figure S1

Captions for Movies S1 and S2

Other Supporting Online Material for this manuscript includes the following:

Movies S1 and S2

Supporting online material

Hydrogen subsurface penetration on Pd(100) with $\Theta_H = 0.5$ coverage

The snapshots presented in Fig. 4 have been taken from a ab initio molecular dynamics run of a hydrogen molecule impinging on a Pd(100) surface with an initial hydrogen coverage of $\Theta_H = 0.5$ monolayer within a (3×2) unit cell. In the animation S1 `H2Pd100_3x2_ThetaH05.mpg` provided at the URL XX a sequence of the whole trajectory from $t = 850$ fs to $t = 1200$ fs is shown capturing the process of the concerted subsurface penetration.

Caption for movie S1:
Sequence of an ab initio molecular dynamics trajectory capturing the concerted subsurface penetration illustrated by the snapshots shown in Fig. 4.

Hydrogen subsurface penetration on Pd(100) with $\Theta_H = 0.75$ coverage

In this section we present the results of NEB calculations for one hydrogen atom entering to the Pd(100) subsurface for a H_2 molecule on a 2×2 cell of the surface with an initial hydrogen coverage of $\Theta_H = 0.75$. The reaction pathway shown in Fig. S1 starts with the H_2 molecule 3.52 Å above the surface ($H_{2,g}$ state) from which the molecule can reach states very similar to the $H_{2,ad}$ and $H_{br}H_{ad}$ ones shown in Fig. 5, without encountering any activation energy barrier. Note that in the present case (initial coverage $\Theta_H = 0.75$ and 2×2 cell), it is not possible to form the $H_{ad}H_{ad}$ intermediate state corresponding to a full hydrogen overlayer on Pd(100) as in Fig. 5 because there are five H atoms and only four surface adsorption sites available per cell.
Still, similarly to the case analysed in Fig. 5, the activation energy barrier between the $H_{br}H_{ad}$ and $H_{sub}H_{ad}$ states is ~ 0.16 eV, being the energy of the transition state ~ 0.35 eV below the zero energy reference level, corresponding to the molecule far form the initially precovered surface.
This relatively small activation energy barrier for hydrogen penetration to the subsurface is a consequence of a concerted motion through which the H_{ad} atom enters the subsurface site at the same time that the H_{br} atom refills the emptied fourfold hollow adsorption site. A movie showing the sequence of configurations along the minimum energy reaction pathway shown in Fig. S1 can be visualized in the animation S2 `H2Pd100_2x2_ThetaH075.mp4` .

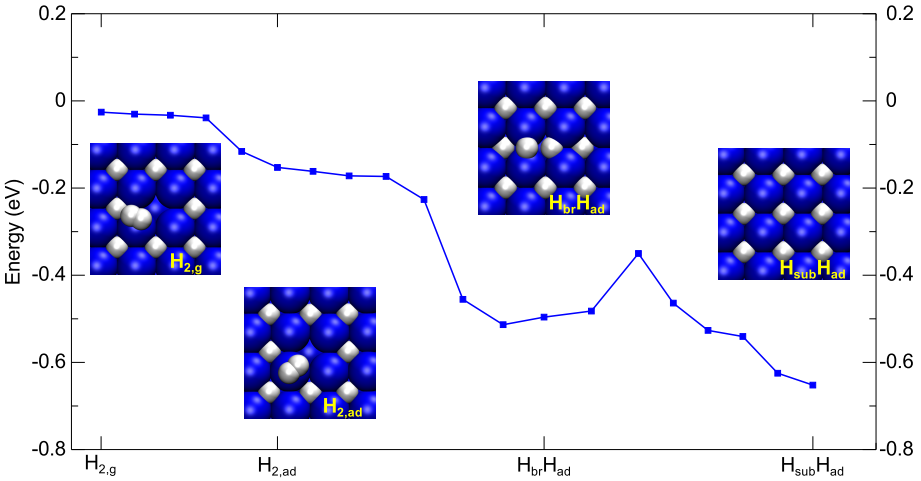

FIG. S1: Reaction pathway for hydrogen subsurface penetration upon H_2 adsorption over Pd(100) with $\Theta_H = 0.75$ initial coverage. The configuration $H_{2,g}$ corresponds to the molecule in the gas phase, $H_{2,ad}$ is an analogue structure to the molecular precursor state in the $c(2 \times 2)$H/Pd(100) surface (see Fig. 5 in main article), $H_{2,diss}$ is the dissociated and adsorbed state with lower energy, and in $H_{sub}H_{ad}$ there is a monolayer of H adatoms at the hollow sites with an additional H atom in a subsurface site per (2×2) unit cell.

Caption for movie S2:
Configurations and energies along the minimum energy reaction pathway for the concerted subsurface penetration of a H_2 molecule on a 2×2 cell of Pd(100) with an initial hydrogen coverage of $\Theta_H = 0.75$.